Title

Effect of storms during drought on post-wildfire recovery of channel sediment dynamics and habitat in the southern California chaparral, USA

Permalink

Authors

Florsheim, Joan L
Chin, Anne
Kinoshita, Alicia M
et al.

Publication Date

2017

DOI

10.1002/esp.4117

A final version of this paper was published in the journal Earth Surface Processes and Landforms http://dx.doi.org/10.1002/esp.4117

Please cite as: Florsheim, J.L., Chin, A., Kinoshita, A.M., and Nourbakhshbeidokhti, S. (2017) Effect of storms during drought on post-wildfire recovery of channel sediment dynamics and habitat in the southern California chaparral, USA. Earth Surf. Process. Landforms, doi: 10.1002/esp.4117.

Effect of storms during drought on post-wildfire recovery of channel sediment dynamics and habitat in the southern California chaparral, USA

Joan L. Florsheim[1], Anne Chin[2]; Alicia M. Kinoshita[3]; Samira Nourbakhshbeidokhti[3]

[1]*Earth Research Institute, University of California, Santa Barbara, California, 95616 USA*
E-mail: florsheim@eri.ucsb.edu

[2]*Department of Geography and Environmental Sciences, University of Colorado, Denver, Colorado, 80217, USA*

[3]*Department of Civil, Construction and Environmental Engineering, San Diego State University, San Diego, California, 92182, USA*

ABSTRACT: Current global warming projections suggest a possible increase in wildfire and drought, augmenting the need to understand how drought following wildfire affects the recovery of stream channels in relation to sediment dynamics. We investigated post-wildfire geomorphic responses caused by storms during a prolonged drought following the 2013 Springs Fire in southern California (USA), using multi-temporal Terrestrial Laser Scanning and detailed field measurements. After the fire, a dry-season dry-ravel sediment pulse contributed sand and small gravel to hillslope-channel margins in Big Sycamore Creek and its tributaries. A small storm in WY 2014 generated sufficient flow to mobilize a portion of the sediment derived from the dry-ravel pulse and deposited the fine sediment in the channel, totaling ~0.60 m^3/m of volume per unit length of channel. The sediment deposit buried step-pool habitat structure and reduced roughness by over 90%. These changes altered sediment transport characteristics of the bed material present before and after the storm; the ratio of available to critical shear stress (τ_o/τ_c) increased by five times. Storms during WY 2015 contributed additional fine sediment from tributaries and lower hillslopes and hyperconcentrated flow transported and deposited additional sediment in the channel. Together these sources delivered sediment on the order of six times that in 2014, further increasing τ_o/τ_c. These storms during multi-year drought following wildfire transformed channel dynamics. The increased sediment transport capacity persisted during the drought period characterized by the longer residence time of relatively fine-grained post-fire channel sedimentation. This contrasts with wetter years, when post-fire sediment is transported from the fluvial system during the same season as the post-fire sediment pulse. Results of this short-term study highlight the complex and substantial effects of multi-year drought on geomorphic responses following wildfire. These responses influence pool habitat that is critical to longer-term post-wildfire riparian ecosystem recovery.

Keywords: wildfire, fluvial geomorphology, sediment, dry ravel, drought, habitat

INTRODUCTION

The occurrence of drought and longer and earlier dry seasons associated with global warming (Lenihan et al., 2003; Westerling et al., 2006; Bowman et al., 2009; Turco, 2014; Dennison et al., 2014) and human influences (Mann et al., 2016) could affect the number, size, frequency, timing, and intensity of future wildfires. Environments in semi-arid Mediterranean climates, such as those in southern California, are susceptible to such changes (Keeley and Syphard, 2015; 2016). Typically, sediment supply to stream channels in Mediterranean climates is episodic (Inman and Jenkins, 1999), and in turn may be influenced by altered climate and wildfire regimes. Although aquatic habitat and species native to southern California's chaparral ecosystems are resilient to episodic annual drought (Verkaik et al., 2013a), the geomorphic adjustments that alter the physical attributes interacting with aquatic ecology during multi-year drought following wildfire disturbance has not yet been investigated.

Wildfire elevates sediment supply by burning vegetation that stabilizes weathered sediment on hillslopes (Shakesby and Doerr, 2006; Moody et al., 2013). In steep semi-arid chaparral basins, dry ravel is a dominant hillslope process by which weathered sediment is transported downslope by gravity (Anderson, et al., 1959; Krammes, 1965; Rice, 1982; Florsheim et al., 1991; DiBiase and Lamb, 2013; Wohlgemuth, 2015). Therefore, in steep chaparral environments, wildfire initiates a dry ravel sediment pulse to hillslope-channel margins in tributaries and in main channels (Florsheim et al., 1991; 2016; Gabet, 2003; Lamb et al., 2011; 2013). In steep step-pool stream channels, sediment contributed by dry ravel that consists of gravel and smaller sediment contrasts with the coarser cobble and boulder pre-fire channel bed material (Florsheim et al., 1991). Geomorphic responses to these landscape-scale sediment pulses during years with moderate rainfall include mobilization and then temporary deposition in channels before material is transported through the system. Morphology recovers to its pre-fire state, creating a sediment disturbance with less than a one-year residence time (Florsheim et al., 1991; Keller et al., 1997). Thus, during non-drought storm seasons, fire-related sediment supply is readily transported, instead of stored, because rainfall and runoff are adequate to transport material delivered through dry ravel and other processes. In contrast to these fluvial channel responses to fire, debris flows are common in steeper first-order tributaries (Wells, 1987; Wells et al., 1987; Cannon et al., 2001; Staley, et al., 2013; Kean et al., 2011; Prancevic, et al., 2014).

The resilience of fire-prone ecosystems depends in part on the effect of the fire in creating diverse environments that may facilitate range shifts of species, such that in some cases, fire may be a factor that helps some ecosystems respond to climate change (Moritz and Knowles, 2016). However, from the standpoint of the riparian ecosystem, elevated inputs of sediment to stream channels after wildfire degrade aquatic habitat and impact organisms (e.g., Bozek and Young, 1994; Rinne, 1996; Gamradt and Kats, 1997; Pettit and Naiman, 2007). Pools in steep step-pool channels, in particular, are often important habitats (O'Dowd and Chin, 2016) for a range of organisms. Fine sediment filling pools decreases the heterogeneity of such habitats (Minshall et al., 1997). Prior work shows that ecosystems disturbed by wildfire often recover when sediment sources decline as vegetation reestablishes (Robichaud et al., 2009). The magnitude of the post-fire responses, however, may vary by biogeographic regions (Verkaik et al., 2015) and the inherent resilience, diversity, and stability of the ecosystem (Justus, 2008; Mori, 2016; Oliver et al., 2016). Post-fire climate patterns – whether extended drought or extreme rainfall events – pose an additional disturbance at a seasonal or inter-annual temporal scales that superimposes on the longer-term consequences of fire impacts (Bixby et al., 2015). Because a large disturbance such as wildfire may render fluvial systems sensitized to small climatic events, our understanding is incomplete with respect to the sequence of disturbance impact and recovery, especially during prolonged drought such as is characteristic of southern California.

We hypothesize that drought persisting after a wildfire alters the magnitude and timing of geomorphic responses with respect to mobilization and transport of the elevated post-wildfire sediment supply, and that these alterations to sediment dynamics significantly affect ecosystem recovery. To test the hypothesis, we investigated morphodynamics in a steep southern California chaparral fluvial system during the multi-year drought that began in 2012 in the western USA, one of the most severe recorded (Diaz and Wahl, 2015; Diffenbaugh et al., 2015). Our findings illustrate the effects of drought on post-fire sediment dynamics in stream channels. They also contribute toward prediction and management of wildfire disturbances and recovery in steep chaparral landscapes. Finally, results of this work highlight the complex and substantial effects of climate variability on fluvial systems after wildfire.

STUDY AREA

The study area lies within the Santa Monica Mountains, the southern-most range of the steep, rugged Transverse Ranges in southern California's coastal Mediterranean region. The Santa Mountains are comprised of Cenozoic marine sandstone and shale layers (Yerkes and Campbell, 1980, Dibblee and Ehrenspeck, 1990a; 1990b). We investigated post-wildfire sediment dynamics in a study reach in the headwaters of Big Sycamore Creek, an ephemeral second-order alluvial channel with 14 first-order tributaries in the channel network (upstream drainage area ~1.8 km^2; Figure 1). The Big Sycamore Creek study area lacks floodplains such as are present lower in the fluvial system, and is therefore characterized by a high degree of connectivity between steep hillslopes and the channel. The present research builds on prior work that investigated step-pool dynamics (Chin, 1999; 2002) and extends prior analysis in the lower portion of the study reach regarding hillslope dry-ravel dynamics following the 2013 Springs Fire (Florsheim et al., 2016). In channels with steps and pools, such as Big Sycamore Creek, coarse bed material tends to be mobile only during high magnitude flows (Chin, 1998) with a low sediment supply between wildfires that is limited by soil production rates (Lamb et al., 2011). Over the past 1,000 years, wildfire in the study area has a recurrence interval of ~36 yr (National Park Service, 2015). The Springs Fire burned ~100 km^2 including 85% of Big Sycamore Canyon with moderate severity (National Park Service, 2013).

Southern California typically experiences a variable precipitation regime. The majority of rain usually falls between October and May; whereas, June through September are usually dry months. However, the seasonal drought duration sometimes lasts 10 months of the year. A multi-year drought began in the southwestern United States of America (USA) during water year (WY) 2012. Warm, dry Santa Ana winds, often associated with California wildfires (Davis and Michaelson, 1995; Moritz et al., 2010; Keeley, 2015) combined with the drought and set conditions for the May 2-6 2013 Springs Fire. The Palmer Drought Severity Index (PDSI), a prominent index of meteorological drought (Heim, R.R. Jr., 2002), utilizes precipitation and temperature data to estimate relative dryness. The PDSI (Figure 2A), showing the relationship of the Springs Fire occurring during the second year of the drought, fits the pattern relating an extreme moisture deficit triggered by drought and large fires that can occur in the southwestern USA (Swetnam and Betancourt, 1998; Westerling et al., 2003).

Nevertheless, some storms occurred during the extreme drought period continuing after the Springs Fire (Figure 2B; Ventura County Water Protection District; rainfall depths measured hourly; ID 513 operated since 18 Feb 2014). One small storm occurred the first post-fire winter during WY 2014 (27 Feb – 2 Mar). Over five days, this storm generated 74.1 mm of rainfall (maximum rainfall depth measured over a one hour period = 9 mm). During the second post-fire winter, WY 2015, a two-day storm with smaller magnitude but higher intensity occurred (11-12 Dec 2014: 63.0 mm, maximum depth measured over a one hour period = 30 mm). During the third post-fire winter, WY 2016, two storms occurred (4-7 Jan: 64.2mm and 6-8 Mar: 38.0 mm, maximum depths measured over a one hour period = 33 mm and 36 mm, respectively).

METHODS

We collected field data in Big Sycamore Creek over a two-year period following the 2013 Springs Fire. We distinguish a lower and upper portion of a contiguous study reach; all of the profile, grain size, and dry ravel measurements were conducted in the entire reach. Additional topographic data collected using Terrestrial LiDAR Scanning (TLS) in the lower portion of the study reach is discussed in the subsequent section. To explore annual precipitation trends over a longer record than is available from the local Rancho Sierra Vista rain gage (Figure 1) we compared the local storm rainfall totals to the mean of the longer-term rainfall record using satellite-based data. To accomplish this, we extracted the PRISM (parameter-elevation regressions on independent slopes model; Daly 1994; 1997; 2002) precipitation dataset for Big Sycamore Canyon (120 year dataset available from WY 1896 -2016 (WestWide Drought Tracker (WWDT); lat: 34.14207; long: -118.94142; http://www.wrcc.dri.edu/wwdt/time/).

Three thalweg longitudinal profiles and grain size measurements included: before and after the 2014 storm, and after the 2015 storms. The survey and grain size distribution data facilitated quantification of reach-scale channel changes that influence sediment transport. Grain size (D_s) between boulder steps was measured using the median diameter of 100 randomly selected grains (Wolman, 1954). The maximum grain diameter of steps (D_{max}) was estimated using the five largest boulders present (Chin, 1999). Sediment sorting was estimated as the standard deviation ($\sigma(D_s)$) of the sample grain sizes, where sorting increases as $\sigma(D_s)$ decreases. We compared form roughness as step height (H_s), spacing (λ_s) (Egashira and Ashida, 1991), and grain roughness (D_{84}) (Aberle and Smart, 2003) before and after the storms.

Volumes of dry ravel deposits representing sediment supply from hillslope erosion during and immediately following the fire were measured following the approach used in Florsheim et al. (2016) to evaluate short-term changes in hillslope dry-ravel processes. Field measurement of dry ravel deposits included height (*h*) from the base of the deposit in the channel margin to the top on the hillslope, and length (*l*) along the longitudinal profile of the channel using a stadia rod and tape measure, respectively; depth (*d*) of each deposit was measured perpendicular to height using a steel rebar probe. The dry-ravel deposit volume calculation used geometric relationships depending on the shape of the deposit, generalized as one half an (upside-down) cone ((V_{ci}): $V_{ci} = (1/6)\ \pi\ r^2\ h$ where depth, measured in the location corresponding to the deepest portion of the deposit, replaces the cone radius, *r*), or quasi-rectangles ($V_{ri} = A\ d$ where A *is* the surface area of the deposit (*w h*)). The total volume V_T of sediment stored in the *n* dry-ravel deposits for the reach is: $V_T = \Sigma\ V_{ci} + \Sigma$

V_{ri} *where i = 1…n*. In the present study, dry-ravel volumes reported in Florsheim et al. (2016) for the lower portion of the study reach are extended upstream through the burned area.

Changes in fluvial transport capacity resulting from post-wildfire geomorphic adjustments were estimated by comparing shear stress available during storm flows, $\tau_o = \gamma R S$, to the critical shear stress needed to transport the predominant size of sediment, $\tau_c = \tau_* (\rho_s - \rho_w) g D_{84}$; where γ is the specific weight of water, *R* is the hydraulic radius determined from high water marks, S is assumed equivalent to the bed slope over the reach length, τ_* is the dimensionless Shields stress $\tau_* = 0.15 S^{0.275}$ (Recking et al., 2012) that allows for changes in channel slope caused by sediment deposition, and ρ_s and ρ_w are the densities of sediment and water, respectively. For sediment entrainment to occur, τ_o must be larger than τ_c, thus the ratio τ_o/τ_c must exceed 1.0 before bed material transport occurs.

Terrestrial LiDAR Scanning (TLS) Datasets and Uncertainty Analysis

Channel topography of the lower portion of the study reach was documented with Terrestrial Laser Scanning (TLS). The first TLS scan ("before 2014 storm") took place in October 2013 before fire-related morphologic channel changes occurred, followed by the second scan in April 2014 ("after 2014") storm." Channel topography was documented using methods similar to those detailed in other post-fire investigations of steep tributaries, hillslopes, and piedmonts (Staley et al., 2014; Wester et al., 2014; Orem and Peltier, 2015; Rengers et al., 2016). The TLS scans were collected by UNAVCO (formerly called University NAVSTAR Consortium; www.unavco.org) using a Riegl VZ-400 scanner, including 14 scan positions in the dry study reach. Registration and alignment of Big Sycamore Creek scans followed methods outlined in Williams et al. (2012) and are described in detail in Florsheim et al. (2016). Steps taken to process the raw TLS point cloud data included: 1) an octree method to provide a homogenous point density that recursively subdivides the point cloud into the octree (cell size 0.1 m) with each resulting octant containing a data point; 2) filtering and removing vegetation from the point clouds; and 3) triangulating the processed point cloud to create bare earth digital elevation models (DEMs) of the study reach. The DEMs provided a guide to identify active channel boundaries. RiScan Pro 2.0.3 was used to: 1) clip the surfaces to exclude hillslopes and dry ravel deposits before analysis of relative volume changes in the active channel; 2) to process TLS point clouds; 3) generate cross sections used in the uncertainty analysis; and 4) compute the volumetric difference (m^3) between the triangulated surfaces for the before- and after-storm TLS scans. Elevation differences, indicating erosion and deposition, were estimated between the before- and after-storm images using CloudCompare.

Error is inherent in change detection using TLS (Wheaton et al. 2010), where uncertainty in the DEM surfaces versus the actual ground surface results from combined sources such as LiDAR instrument inaccuracy, registration inaccuracy, point coverage gaps, the octree method of filtering, and topographic filtering that removes irregular topography or does not remove all the non-bare earth points. Errors typically attributed to georeferencing are not incorporated within the dataset because registration for the initial point cloud in the Big Sycamore study reach was based on identifiable physical features, not global positioning system (GPS). To estimate the uncertainty within each TLS scan, we selected and compared the x, y, and z coordinates of identifiable areas on 10 large boulders (D_{50} ranging between 0.7 m and 4.4 m with an average D_{50} of the 10 boulders equal to 1.38 m) that did not move between the 2013 and 2014 TLS campaigns (Figure 3A). Within these areas, differences in the number of points in the point cloud data in the 2013 and 2014 scans make a point-by-point comparison challenging. However, to avoid bias in the uncertainty analysis, the boulder areas used in the uncertainty analysis include some zones with low point density. Thus, for each rock, we randomly sampled a 0.5 m by 0.5 m area and averaged the x, y, and z for 2013 and 2014. Positional errors in the horizontal components (x and y) have negligible influence on the vertical surface difference in most fluvial systems (Wheaton et al. 2010). Nevertheless, we report the comparison of the horizontal components and vertical component (elevation, z) of each sample area on the 10 boulders to quantify spatial differences between the two point clouds that may influence the estimate of volumetric change between the 2013 and 2014 scans (Table 1). The comparison yields average absolute difference of 0.006 m and 0.007 m for x and y, respectively (Table 1) and an average elevation difference (Δz) of 0.008 m. This estimate encompasses the manufacturer error estimate of 0.005 m.

We utilized the triangulated surfaces instead of smoothing the triangulated surfaces to avoid introducing error associated with interpolation and smoothing (systematic error ~0.1 m in comparison of the smoothed surface with corresponding points from the point cloud). To determine error introduced in creating the triangulated surface itself, we compared the triangulated surfaces to the corresponding points in the TLS point cloud. To accomplish this, cross sections every ~12 m throughout the lower study reach were extracted using RiScan Pro (Figure 3B). The elevations of the triangulated surfaces compared well to the corresponding elevation of the TLS points along each cross section with average root mean square errors (RMSE) less than 1.0 cm for both scan campaigns (Table 2). The average bias, a measure of error that indicates systematic difference in the relative elevations of the triangulated surfaces and TLS points is minimal (Table 2).

To further minimize error in determining the volumetric difference between the pre- and post-storm active channel triangulated surfaces, we removed areas with no points before calculating the volumetric difference. To do this, the plotted spatial distribution of available points in the combined point clouds in the study reach were used to delineate gaps in the point coverage caused by the shadow below the instrument and irregular topography not filled in by adjacent scanner setups. About 12% of the total area scanned was excluded from the analysis due to insufficient point coverage.

Based on the tests described above, we report the maximum elevation error calculated by differencing the 2013 and 2014 TLS scans as the square root of the sum of the squared error from the 2013 and 2014 triangulation of the TLS scans ($0.0056^2 + 0.0054^2$) and Δz (0.008^2), or ±0.011 m over the entire active channel scanned. This error translates to a maximum estimated uncertainty in the volumetric change estimate of ~16% of the total volume.

RESULTS

Magnitude, Frequency, and Duration of the Drought beginning in 2012

Analyzing the PRISM precipitation dataset for Big Sycamore Canyon (Figure 4) provides a longer-term climate context for the storms occurring during the drought persisting following the Springs Fire. Overall, variability characterizes the 1896-2016 precipitation regime. A comparison of the long-term mean (~416 mm/yr) to annual rainfall measured at Rancho Sierra Vista gage highlights the drought-years during the study period (Figure 4). Average annual rainfall during WY 2014, WY 2015, and WY 2016 was ~39%, ~64%, and 39%, respectively, of the long-term mean.

To consider how typical the post-fire responses investigated in this study were in Big Sycamore Canyon, we report the duration of drought conditions by further analyzing the PRISM data, with years when rainfall is at least 20% below the long-term average corresponding to the mild-extreme PDSI drought classifications. The frequency of the number of consecutive years of drought of various durations indicates that most (61%) of the dry years are preceded and followed by wetter years; thus, having a 1-year drought duration (Figure 4). The frequency of two- and three-year drought durations is 20% and 10% of the dry years, respectively. Four-year (WY 1948-1951) and 5-year (WY 2012-2016, to date) drought durations have occurred only once during the151-year period of record, each comprising only 3% of dry years (Figure 4).

Sediment Deposition during the 2014 Storm

After the 2013 Springs Fire, before the WY 2014 storm, Big Sycamore Creek was characterized by coarse cobble, gravel, and boulder bed material and step-pool structure (Table 3; Figure 5) morphologically identical to the pre-fire condition with the exception of ash remaining where vegetation burned. The WY 2014 storm substantially altered pool depths, step heights, and grain sizes. Fluvial transport and deposition of sediment supplied by the wildfire-related dry-ravel pulse during the flow generated by the small WY 2014 storm buried a considerable portion of the pre-existing channel bed, including step-pool morphology; all of the pools filled and boulders in few steps remained partially exposed (Table 3; Figure 5), such that channel morphology altered from step-pool to a relatively planar bed. Comparisons of longitudinal profiles surveyed before and after the storms shows that the depth of fill varied from a few centimeters where sediment filled spaces between exposed cobbles protruding from the bed, to as much as 1.05 m where the sediment filled pools (Figure 6). Fill depth averaged ~0.41 m along the thalweg profile of the study reach; average channel slope before and after the storm remained the same, at 0.048.

The volume of sediment deposited in the active channel, calculated by comparing TLS data before and after the WY 2014 storm in the lower portion of the study reach (Figure 7), equaled ~0.60 m^3/m (~106.0 m^3 over an analyzed length of 176.4 m). Field observations documented four sources for the fill: 1) dry ravel directly to the channel margin, poised for transport; 2) rills, in dry-ravel derived sediment stored on hillslopes, discharging directly to the main channel; 3) tributary contributions; and 4) transport from the main channel upstream of the study reaches. The initial dry-ravel sediment pulse released after the 2013 Springs Fire formed dry-ravel deposits along channel margins measured in the contiguous lower and upper portion of the study reach and upstream through the burned zone shortly after the fire stored 0.21 m^3/m of sediment (~107.5 m^3 over a 504 m channel length). Of the total volume within this longer reach, ~70.9 m^3 remained after the 2014 storm, suggesting that 34% was mobilized and transported (comparable to that measured for the lower portion of the reach alone, reported in Florsheim et al., 2016). This sediment eroded from dry ravel deposits accounted for 34% of the volume of the deposit that filled the lower portion of the reach during the 2014 storm.

The other three sources contributing sediment during the 2014 storm—rills, tributaries, and main channel transport from the upstream watershed—likely contributed the remaining sediment in the fill deposit. Small rills observed on lower hillslopes near the head of the lower reach were not measured. Of 14 first-order tributaries, 11 yielded sediment that formed distinct small fans protruding a few meters into the main channel. Flow in the main channel during the same storm then partially eroded these deposits, suggesting that the tributaries quickly responded to the storm before flow subsided in the main channel. The average grain sizes of tributary-derived sediment were D_{50} = 9.3 mm and D_{84} = 26.1 mm (Figure 8a). Field estimates of the volume remaining in fan deposits after erosion by main channel flow during this storm was ~12.8 m^3. Stratigraphy of the main channel deposit included clast support of grains, imbrication, and vertical layering. Surface morphology included braiding on wider portions of the deposit, and high water marks were evident along banks.

Grain size distributions of the active channel bed between steps before the 2014 storm were coarse in contrast to those present after alteration by the sediment deposited during the storm (Figure 8A; Table 3). Average D_{50} and D_{84} decreased by an order of magnitude as a result of the influx of finer sediment that buried the pre-storm bed material. Grain size characteristics illustrate similarity in the fine sediment derived from the post-fire dry-ravel sediment pulse (average D_{84} = 8.6 mm, average σ (D_s) = 3.6 mm (not shown on table 3)) and material that filled the channel during the storm (Figure 8A). The σ (D_s) only decreased by 30% because the tops of boulders were still exposed following the storm (Table 3).

Alteration of bed material characteristics and channel morphology caused by the 2014 deposition decreased roughness (see Figure 5). D_{84} decreased by ~93% (Table 3); form and spill roughness were significantly reduced by burial of the majority of the steps. The active channel appeared relatively smooth after the sediment influx (Figure 8B). These physical characteristics of the bed material and bed structure, including grain size and roughness, increased the ability of flow to mobilize fire-related sediment. The ratio τ_o/τ_c increased significantly after the deposition during the 2014 storm, with available bed shear stress ~five times that needed to transport the sediment supplied to the channel in the storm (Table 3). During the storm, fluvial flow transported the sediment until flow lost capacity as flows receded on the waning limb of the storm hydrograph, and the relatively fine sediment buried the coarser substrate and the step-pool structure.

Sediment Deposition during the WY 2015 Storms

Sediment deposition during the WY 2015 storms increased the channel bed elevation by another ~0.64 m, on average, atop the 2014 deposit (see Figure 6). This sediment in the new deposit, with grain roughness D_{84} = 8.0 mm (Figure 8A, Table 3) and sorting $\sigma(D_s)$ = 3.5 mm (Table 3), buried the majority of the remaining step-pool structure and increased τ_o/τ_c to 13.7 (Table 3). The volume deposited (calculated by projecting a surface through the surveyed profile elevations and calculating the difference between the projected and TLS-derived surfaces) was ~six times the volume of the WY 2014 deposit (621.7 m^3, or 3.5 m^3/m in the 176.4m reach). The same sources active during the 2014 storm provided the additional sediment, albeit in different proportions. First, the remainder (66%) of the total sediment supplied by dry ravel to the main channel margins was mobilized (~71 m^3) and accounted for ~11% of the total fill volume. Contributions from tributary and the upstream channel (that also included material derived from hillslope dry ravel) and abundant rills on lower hillslopes observed in the burned area following the WY 2015 storms likely provided the remainder of the sediment; however, estimates of the volumes for each source are not available. Observations during field reconnaissance after the small WY 2016 storms occurring during the continuing drought, showed only minor changes to the material deposited during the 2015 storms.

A soil pit excavated into the 2015 channel deposit near the mid-point of the lower portion of the study reach showed weak horizontal stratification with poorly sorted gravely sand between layers of gravel, with the long axes of clasts oriented parallel to the flow direction, characteristic of deposition by hyperconcentrated flow. The uppermost 0.06-0.08 m of the 2015 channel deposit exhibited relatively well sorted gravel, and together with a braided pattern on the relatively planar surface in some locations, suggests some reworking by the latest stage of storm flow. Field observations at tributary confluence zones showed cobbles and relatively coarser clasts mixed with finer main-channel sediment.

DISCUSSION

After the 2013 Springs Fire, a dry-ravel pulse supplied fine grained sediment to channel margins, lower hillslopes and tributaries in Big Sycamore Canyon, a steep fluvial system in southern California (Florsheim et al., 2016). Even the relatively small magnitude storms that occurred during the drought following the Springs Fire (39% and 64% of the long-term mean rainfall during WY 2014 and WY 2015, respectively) mobilized the post-fire sediment delivered to Big Sycamore Creek. Although the small WY 2014 storm generated flow and easily mobilized and transported this fine-grained sediment within the stream channel, streamflow was insufficient to transport the volume of sediment downstream. Instead, as the storm ended and flow lost capacity, sediment was deposited—partially burying the coarse-grained, rough, step-pool channel morphology. No other sediment transporting flows occurred during WY 2014. Therefore, the drought-moderated fluvial response exceeded one season, lengthening the residence time of fire-related sediment deposition, and postponing recovery to the pre-fire step-pool channel morphology and associated habitat.

The WY 2015 (11-12 Dec 2014) storm in Big Sycamore Canyon occurred during the continuing drought. The WY 2015 storm was characterized by a lower magnitude and larger intensity rainfall than the event that occurred during the prior winter. The additional large volume of sediment deposition in Big Sycamore Creek during this storm suggests that a substantial supply of fire-related sediment supply was still available after the first post-fire storm season. The sediment was still stored in: 1) tributary and main channel margin dry ravel deposits not already flushed out by the 2014 storm; and 2) weathered sediment mobilized by post-fire dry-ravel processes on hillslopes where vegetation re-growth during the persisting drought was not sufficient to re-stabilize available material. Thus, sediment availability from both drought-moderated sources provided the post-wildfire supply to the main channel during the second winter after the fire.

The sediment/water ratio during the WY 2015 storm flow likely depended on the spatial variability and timing of sediment and water inputs from multiple sources. These sources include erosion of channel-margin dry-ravel deposits and rill inputs from dry ravel deposits stored on lower hillslopes. In steeper first-order tributaries, debris flows likely occur during such storms (*sensu* Gabet et al., 2008; Prancevic, et al., 2014). Nonetheless, even small fluvial and hyperconcentrated flows generated from small storms are sufficient to mobilize and transport fire-related fine-grained material within main channels. If transport capacity decreases before the large influx of sediment supplied is transported downstream, these storm flows then deposit a large volume of sediment. We infer that storm flows with magnitude greater than the threshold for transport of the fine sediment did not have sufficient duration to flush the large volume of sediment supplied from the system. Observations of minor channel changes during the WY 2016 storms (with smaller magnitudes but larger depths measured over a one hour period than those that occurred during the 2015 storm), suggest that the post-wildfire supply may have been depleted or stabilized.

These geomorphic responses to wildfire-related increases in sediment supply during the persisting drought, contrast with previously documented flushing of post-wildfire sediment during the winter storms following wildfire. During relatively wet winter seasons, storm flows easily transported and removed the fine sediment supplied by dry ravel (Scott, 1971; Laird and Harvey, 1986; Campbell et al., 1987; Florsheim and Keller, 1991; Keller et al., 1997; 2015). These prior studies indicate that, during wet storm seasons following wildfire, the sediment contributed via the post-wildfire sediment pulse is not stored in the long-term. Rather, sediment is mobilized, deposited, and then flushed from the system within one storm season. In contrast when small storms during extended drought are unable to flush out fire-related sediment from fluvial systems, the increased residence time of the sediment significantly alters the channel dynamics. Further work is warranted to document inter-relationships among vegetation re-growth that stabilizes weathered sediment on hillslopes, sediment supply, and climate variability.

Persisting post-wildfire sedimentation changes channel dynamics and disrupts ecological interactions within steep channels, where the characteristic alternating steps and pools provide heterogeneous aquatic habitats (Scheuerlein, 1999; O'Dowd and Chin, 2016) for a variety of organisms. Step-pool habitat is significant in a range of environments. For example, step-pool structure supports salmonids in the pacific northwest, USA (Montgomery et al., 1999), tailed frogs in northwest California (Welsh and Ollivier, 1998), and treefrogs and newts in the Santa Monica Mountains of southern California (Gamradt and Kats, 1997; Kerby and Kats, 1998; Delaney and Riley, 2013; 2014). The post-fire sediment filling pools decreases the heterogeneity of habitats (Minshall et al., 1997) while providing local conditions that may attract organisms tolerant to the disturbance, changing ecological relationships (e.g., Andradi, 1999; Kaller and Hartmann, 2004).

In Big Sycamore Canyon, aquatic herptofauna (Pacific treefrog, California treefrog, and California newt) were affected by the severe drought prior to the Springs Fire (Delaney and Riley, 2013; 2014). These organisms continue to be affected by the combination of continuing drought and the transformation of the physical channel habitat (Delaney and Riley, 2015; Delaney Pers. Comm., National Park Service, 2016). Drought influences post-wildfire ecological recovery by decreasing rainfall necessary to generate channel flows necessary to flush fire-related sediment from pools. Moreover, infiltration into the post-wildfire sediment deposit leading to subsurface instead of surface flows likely compounds the lack of moisture required for riparian herptofauna to breed. The persistence of these changes influences the recovery of organisms following wildfire. We infer that the longer-term ecological consequence of post-wildfire sedimentation arising from storms during multi-year drought is closely tied to the longevity of the drought.

In this study, both the wildfire and the prolonged drought serve as disturbances to the fluvial system. Instead of facilitating recovery of the fluvial system, small magnitude storms during prolonged drought in southern California compounded the negative impacts of the wildfire. Similar negative impacts were recorded following wildfire and eight years of drought in Australia, where combined fire and drought disturbances reduced resilience of macroinvertebrate communities (Verkaik et al., 2013b). These studies suggest that the negative impacts of wildfire disturbance on habitat and stream ecology could be attenuated or compounded according to subsequent climate patterns, and therefore, influence the timeframes and pathways of recovery in ecological habitat and communities.

Although a drought duration of five years has only occurred once in the ~150 year historical record in southern California, Holocene paleo-drought in the region has lasted multiple decades or even centuries (Malamud-Roam et al., 2006; 2007). Therefore, if drought becomes more prevalent, it follows that the short-term (multi-year) drought-moderated post-wildfire geomorphic responses such as recorded in Big Sycamore Canyon will likely recur, and that these responses may persist over longer durations. Even with geomorphic recovery when the drought ends, the longer-term consequence of disturbance such as prolonged sedimentation to riparian ecology may be more complex. This complexity may be especially acute in fragmented ecosystems (M. Witter, Pers. Comm., National Park Service, 2015) such as are present in the growing areas characterized as the wildland-urban interface.

CONCLUSIONS

Field studies during a multi-year drought persisting after wildfire in a southern California chaparral fluvial system yield the following conclusions. First, the initial landscape-scale dry-ravel sediment pulse released after the 2013 Springs Fire from hillslopes to channel margins was poised for transport by stream flows the following winter. Second, a small storm the following winter (WY 2014) generated flow that transformed channel dynamics and morphology. Fine sediment derived from partial erosion of dry ravel deposits and other sources was mobilized and transported until transport capacity decreased below the threshold of mobility—the deposition of sediment buried step-pool morphology. Third, a reduction in grain size, increase in sorting, and loss of morphologic structure and physical habitat occurred due to deposition in the small WY 2014 storm, with residence time that lasted longer than one winter. These changes were magnified by additional sedimentation during WY 2015 storms, and they still persist following WY 2016.

When post-fire dry ravel processes deliver a large volume of fine sediment to stream channels, small storms during drought generate flows that appear incapable of flushing the elevated sediment supply out of the system. Small storms during multi-year drought increase the residence time of sediment deposition. This prolonged drought-moderated residence time impedes the breeding activity of riparian herptofauna. Although the post-wildfire dynamics reported here are short-term with respect to geological processes; they may have long-term impacts to riparian ecology as they prolong geomorphic disturbances to physical habitat. This significant impact to post-wildfire recovery may become more prevalent in Mediterranean systems due to increases in predicted droughts associated with warming climates. Results from this study add to our knowledge regarding the possible range of post-wildfire geomorphic responses in relation to climate variability. This knowledge is needed to predict how fluvial systems will recover following wildfires in the future.

ACKNOWLEDGEMENTS

This work was funded by NSF-RAPID Awards EAR-1359734 and EAR-1359730, SDSU faculty research funds. TLS was conducted by UNAVCO through the NSF Awards. Logistical support was provided by the National Park Service and California State Department of Parks and Recreation. We thank Rune Storesund for preliminary TLS analysis; Linda O'Hirok, Edward Keller, Marti Witter, and Katy Delaney for valuable discussion; Balance Hydrologics for use of a sieve shaker. We appreciate feedback on a previous version of this manuscript from anonymous reviewers. Excellent field assistance was provided from students at the University of California at Santa Barbara: Michael Ackel, Thomas Block, Michael Chan, Karla Cortes, Whitney Jones, and Keitasha Royale; at Cal State Channel Islands:

Alex Gaskill and Ariana Ornellas; and at Harvard-Westlake Academy: Kelly Loeb.

REFERENCES

Aberle, J. Smart, G.M., 2003.The influence of roughness structure on flow resistance on steep slopes. Journal of Hydraulic Research 41(3): 259-269.

Anderson H., Coleman G., Zinke, P.J., 1959. Summer slides and winter scour: dry-wet erosion in southern California mountains. US Department of Agriculture Forest Service, Pacific Southwest Forest and Range Experimental Station, Technical Paper PSW-36, 12 p.

Angradi, T.R., 1999. Fine sediment and macroinvertebrate assemblages in Appalachian streams: A field experiment with biomonitoring applications. Journal of the North American Benthological Society 18: 49-66.

Bixby, R.J., Cooper, S.D., Gresswell, R.E., Brown, L.E., Dahm, C.N., Dwire, K.A., 2015. Fire effects on aquatic ecosystems: an assessment of the current state of the science. Freshwater Science 34(4): 1340-1350.

Bowman, D.M., Balch, J.K., Artaxo, P., Bond, W.J., Carlson, J.M., Cochrane, M.A., D'Antonio, C.M., DeFries, R.S., Doyle, J.C., Harrison, S.P. Johnston, F.H., 2009. Fire in the Earth system. Science 324(5926): 481-484.

Bozek, M.A., Young, M.K. 1994. Fish mortality resulting from delayed effects of fire in the Greater Yellowstone Ecosystem. Great Basin Naturalist 54: 91–95.

Campbell, A.G., Wohlgemuth, P. M., and Wells, W.W., 1987. Post-fire response of a boulder bed channel, In Erosion and Sedimentation in the Pacific Rim. International Association of Hydrological Sciences Publication 16S, p. 277-278.

Cannon, S.H., 2001. Debris-flow generation from recently burned watersheds. Environmental and Engineering Geoscience 7: 321–341.

Chin, A., 1998. On the stability of step-pool mountain streams. The Journal of Geology 106: 59-69.

Chin, A., 1999. The morphologic structure of step-pools in mountain streams. Geomorphology 27: 191-204.

Chin, A., 2002. The periodic nature of step-pool mountain streams. American Journal of Science 302: 144-167.

Daly, C., Neilson, R. P., Phillips, D. L., 1994. A statistical topographic model for mapping climatological precipitation over mountainous terrain. Journal of Applied Meteorology 33: 140-158.

Daly, C., Taylor, G., Gibson, W., Ams, 1997. The PRISM approach to mapping precipitation and temperature. 10th Conference on Applied Climatology, 10-12.

Daly, C., Gibson, W. P., Taylor, G. H., Johnson, G. L., Pasteris, P., 2002. A knowledge- based approach to the statistical mapping of climate. Climate Research 22: 99-113.

Davis, F.W., Michaelson, J., 1995. Sensitivity of fire regime in chaparral ecosystems to global climate change. In Moreno, J.M. Oechel, W.C., eds., Global Change and Mediterranean-Type Ecosystems, Ecological Studies, Vol. 117, Springer NY., p. 435–456.

Delaney, K.S., Riley, S.P., 2013. Monitoring Aquatic Amphibians and Invasive Species in the Mediterranean Coast Network, 2012 Project Report. Santa Monica Mountains National Recreation Area. Natural Resource Data Series NPS/MEDN/NRDS—2013/579, 12 p.

Delaney, K.S., Riley, S.P., 2014. Monitoring Aquatic Amphibians and Invasive Species in the Mediterranean Coast Network, 2012 Project Report. Santa Monica Mountains National Recreation Area. Natural Resource Data Series NPS/MEDN/NRDS—2014/715, 11 p.

Delaney, K.S., Riley, S.P., 2015. Monitoring Aquatic Amphibians and Invasive Species in the Mediterranean Coast Network, 2012 Project Report. Santa Monica Mountains National Recreation Area. Natural Resource Data Series NPS/MEDN/NRDS—2016/1144, 18 p.

Dennison, P.E., Brewer, S.C., Arnold, J.D. Moritz, M.A., 2014. Large wildfire trends in the western United States, 1984–2011. Geophysical Research Letters 41(8): 2928-2933.

Diaz, H.F., Wahl, E.R., 2015. Recent California water year precipitation deficits. A 440-year perspective: Journal of Climate 28: 4637–4652, doi:10.1175/JCLI-D-14-00774.1.

DiBiase, R.A. Lamb, M.P., 2013. Vegetation and wildfire controls on sediment yield in bedrock landscapes. Geophysical Research Letters 40:1093-1097 doi:10.1002/grl.50277, 2013.

Dibblee, T.W., Ehrenspeck, H.E., 1990a.Geologic Map of the Point Mugu and Triunfo Pass quadrangles, Ventura and Los Angeles Counties, California. Dibblee Foundation Map DF-29, scale: 1:24000, 1 sheet.

Dibblee, T.W., Ehrenspeck, H.E, 1990b. Geologic Map of the Camarillo and Newbury Park quadrangles, Ventura County, California. Dibblee Foundation Map DF-28, scale: 1:24 000, 1 sheet.

Diffenbaugh, N.S., Swain, D.L., Touma, D., 2015. Anthropogenic warming has increased drought risk in California. PNAS 112(13): 3931-3936.

Egashira, S., Ashida, K., 1991. Flow resistance and sediment transportation in streams with step-pool bed morphology. In Armanini, A., Di Silvio, G. eds., Fluvial Hydraulics of Mountain Regions: Lecture Notes in Earth Sciences 37, Springer, p. 45-58.

Florsheim, J.L., Chin, A., O'Hirok, L.S., Storesund, R., 2016. Short-term post-wildfire dry-ravel processes in a chaparral fluvial system. Geomorphology 252: 32-39. doi.org/10:1016/jgeomorph.2015.03.035.

Florsheim, J.L., Keller, E., Best, D., 1991. Fluvial sediment transport in response to moderate storm flows following chaparral wildfire, Ventura County, southern California. Geological Society of America, Bulletin 103(4): 504-511.

Gabet, E.J., 2003. Sediment transport by dry ravel. Journal of Geophysical Research: Solid Earth 1978–2012: 108(B1).

Gabet EJ, Bookter A., 2008. A morphometric analysis of gullies scoured by post-fire progressively bulked debris flows in southwest Montana, USA. Geomorphology 96: 298-309.

Gamradt, S.C., Kats, L.B., 1997. Impact of chaparral wildfire-induced sedimentation on oviposition of stream-breeding California newts (*Taricha torosa*). Oecologia 110: 546-549.

Heim, R.R. Jr., 2002. A review of twentieth-century drought indices used in the United States. Bulletin of the American Meteterological Society, 83: 1149–1165.

Inman, D.L., Jenkins, S.A., 1999. Climate change and the episodicity of sediment flux of small California rivers. The Journal of Geology 107(3): 251-270.

Justus, J., 2008. Complexity, diversity, and stability. A companion to the philosophy of biology, pp.321-350.

Kaller, M.D., Hartman, K.J., 2004. Evidence of a threshold level of fine sediment accumulation for altering benthic macroinvertebrate communities. Hydrobiologia 518: 95-104.

Kean, J.W., Staley, D.M. Cannon, S.H., 2011. In situ measurements of post-fire debris flows in southern California: Comparisons of the timing and magnitude of 24 debris-flow events with rainfall and soil moisture conditions. Journal of Geophysical Research: Earth Surface, 116(F4).

Keeley, J.E., Syphard, A.D., 2015. Different fire–climate relationships on forested and non-forested landscapes in the Sierra Nevada ecoregion. International Journal of Wildland Fire 24: 27–36.

Keeley, J.E., Syphard, A.D., 2016. Climate Change and Future Fire Regimes: Examples from California. Geosciences 6(3), p.37.

Keller, E.A., Valentine, D.W., Gibbs, D.R., 1997. Hydrological response of small watersheds following the southern California Painted Cave fire of June 1990. Hydrological Processes11: 401-414.

Keller, E.A., Bean, G., Best, D., 2015. Fluvial geomorphology of a boulder-bed, debris-flow-dominated channel in an active tectonic environment. Geomorphology 243: 14-26.

Kerby, J.L., Kats, L.B., 1998. Modified interactions between slalmander life stages caused by wildfire-induced sedimentation. Ecology 79: 740-745.

Krammes, J.S., 1965. Seasonal debris movement from steep mountainside slopes *in* southern California. In Proceedings, Federal Inter-Agency Sedimentation Conference, Jackson, Miss. US Department of Agriculture Miscellaneous Publications 970: 85-88.

Laird, J. R., and Harvey, M. D., 1986. Complex-response of a chaparral drainage basin to fire, In Hadley, R. F., ed., Drainage basin sediment delivery. International Association of Hydrological Sciences Publication IS9, p. 16S-183.

Lamb, M.P., Scheingross, J.S., Amidon, W.H., Swanson, E., Limaye, A., 2011. A model for fire-induced sediment yield by dry ravel in steep landscapes. Journal of Geophysical Research: Earth Surface Vol. 116, F03006, doi:10.1029/2010JF001878, 2011.

Lamb, M.P., Levina, M., DiBiase, R.A., Fuller, B.M., 2013. Slope, roughness and particle-size controls on sediment storage by vegetation in steep bedrock landscapes: Theory, experiments and implications for post-fire sediment yield. Journal of Geophysical Research: Earth Surface, doi:10.1002/jgrf.20041.

Lenihan, J.M., Drapek, R., Bachelet, D. Neilson, R.P., 2003. Climate change effects on vegetation distribution, carbon, and fire in California. Ecological Applications 13(6): 1667-1681.

Malamud-Roam, F., Dettinger, M.D., Ingram, B.L., Hughes, M., Florsheim, J.L, 2007. Holocene climates and connections between the San Francisco Bay estuary and its watershed—A review: San Francisco Estuary and Watershed Science, 5(1), 28 p.

Malamud-Roam, F., Ingram, L., Hughes, M., Florsheim, J., 2006. Holocene Paleoclimate records from a large California estuary system and its watershed region: linking watershed climate and bay conditions. Journal of Quaternary Science Reviews 25(13-14): 1570-1598.

Mann, M.L., Batllori, E., Moritz, M.A., Waller, E.K., Berck, P., Flint, A.L., Flint, L.E., Dolfi, E., 2016. Incorporating anthropogenic influences into fire probability models: effects of human activity and climate change on fire activity in California. PloS one, 11(4), p.e0153589.

Minshall, G.W., Robinson, C.T., Lawrence, D.E., 1997. Post-fire response of lotic ecosystems in Yellowstone National Park U.S.A. Canadian Journal of Fisheries and Aquatic Sciences 54: 2509-2525.

Montgomery, D.R., Beamer, E.M., Pess, G.R., Quinn, T.P., 1999. Channel type and salmonid spawning distribution and abundance. Canadian Journal of Fisheries and Aquatic Sciences 56(3): 377-387.

Mori, A.S., 2016. Resilience in the studies of biodiversity-ecosystem functioning. Trends in Ecology & Evolution 31(2): 87-89.

Moritz, M.A., Knowles, S.G., 2016. Coexisting with Wildfire: Promoting the right kind of fire—and smarter development—is safer and more cost-effective than fighting a losing battle. American Scientist 104(4): 220-227.

Moritz, M.A., Moody, T.J., Krawchuck, M.A., Hughes, M., Hall, A., 2010. Spatial variation in extreme winds predicts large wildfire locations in chaparral ecosystems. Geophysical Research Letters 37, L04801, doi:10.1029.2009GL041735, 2010.

Moody, J.A., Shakesby, R.A., Robichaud, P.R., Cannon, S.H. Martin, D.A., 2013. Current research issues related to post-wildfire runoff and erosion processes. Earth Science Reviews122: 10-37.

National Park Service (NPS), 2013. Burned Area Emergency Response Plan (BAER), Springs Fire, May2-May 12, 2013. National Park Service, U.S. Department of the Interior, Pacific West Region. Report prepared by the National Park Service Springs Fire BAER Team, 216 p.

National Park Service (NPS), 2015. Fire Frequency. Retrieved from: https://www.nps.gov/samo/learn/management/firefrequency.htm.

O'Dowd, A.P., Chin, A., 2016. Do bio-physical attributes of steps and pools differ in high-gradient mountain streams? Hydrobiologia, doi:10.1007/s10750-016-2735-5.

Oliver, T. H., Heard, M.S., Isaac, N.J.B., Roy, D.B., Procter, D., Eigenbrod, F., Freckleton, R., Hector, A., Orme, C.D.L., Petchey, O.L., Proença, V., Raffaelli, D., Blake Suttle, K., Mace, G.M., Martín-López, B., Woodcock, B.A. Bullock, J.M., 2016. A synthesis is emerging between biodiversity–ecosystem function and ecological resilience research: reply to Mori. Trends in Ecology & Evolution 31(2): 89-92.

Orem, C.A., Pelletier, J.D., 2015. Quantifying the time scale of elevated geomorphic response following wildfires using multi-temporal LiDAR data: An example from the Las Conchas fire, Jemez Mountains, New Mexico. Geomorphology 232: 224-238.

Pettit, N.E., Naiman, R.J. 2007. Fire in the riparian zone: characteristics and ecological consequences. Ecosystems 10: 673–687.

Prancevic, J.P., Lamb, M.P., Fuller, B.M., 2014. Incipient sediment motion across the river to debris-flow transition. Geology, doi:10.1130/G34927.1.

Recking, A., Leduc, P., Liebault, F., Church, M., 2012. A field investigation of the influence of sediment supply on step-pool morphology and stability. Geomorphology 139-140: 53-56.

Rengers, F.K., Tucker, G.E., Moody, J.A., Ebel, B.A., 2016. Illuminating wildfire erosion and deposition patterns with repeat terrestrial Lidar. Journal of Geophysical Research: Earth Surface, DOI: 10.1002/2015JF003600.

Rice, R.M., 1982. Sedimentation in the chaparral: How do you handle unusual events? In Swanson F.J., Janda, R.J., Dunne, T., Swanston, D.N., eds. Sediment Budgets and Routing in Forested Drainage Basins, For. Serv. U.S. Dep. Agric., Washington, D.C. p. 39-49.

Rinne, J.N., 1996. Short-term effects of wildfire on fishes and aquatic macroinvertebrates in the southwestern United States. North American Journal of Fisheries Management 16: 653–658.

Robichaud, P.R, Wagenbrenner, J.W., Brown, R.E., Spigel, K.M., 2009. Three years of hillslope sediment yields following the Valley Complex fires, western Montana. Research Paper RMRS-RP-77. USDA Forest Service, Rocky Mountain Research Station, Fort Collins, Colorado, 8 p.

Scheuerlein, H., 1999. Morphological dynamics of step-pool systems in mountain streams and their importance for riparian ecosystems. In: River Sedimentation: Theory and Applications. Proceedings of the Seventh International Symposium on River Sedimentation pp. 205-210.

Scott, K.M., 1971. Origin and sedimentology of 1969 debris flows near Glendora, CA. U.S. Geological Survey Professional Paper 7SO-C, p. 242-247.

Shakesby, R.A., Doerr, S.H., 2006. Wildfire as a hydrological and geomorphological agent. Earth Science Reviews 74: 269–307.

Staley, D.M., Kean, J.W., Cannon, S.H., Schmidt, K.M. Laber, J.L., 2013. Objective definition of rainfall intensity–duration thresholds for the initiation of post-fire debris flows in southern California. Landslides 10(5): 547-562.

Staley, D.M., Wasklewicz, T.A. Kean, J.W., 2014. Characterizing the primary material sources and dominant erosional processes for post-fire debris-flow initiation in a headwater basin using multi-temporal terrestrial laser scanning data. Geomorphology 214: 324-338.

Swetnam, T.W., Betancourt, J.L., 1998. Mesoscale disturbance and ecological response to decadal climatic variability in the American southwest. Journal of Climate, 11: 3128–3147.

Turco, M., Llasat, M, von Hardenberg, J., Provenzale, A., 2014. Climate change impacts on wildfires in a Mediterranean Environment. Climatic Change 125: 369–380.

Verkaik, I., Rieradevall, M., Cooper, S.D., Melack, J.M., Dudley, T.L. Prat, N., 2013a. Fire as a disturbance in Mediterranean climate streams. Hydrobiologia 719(1): 353-382.

Verkaik, I., Prat, N., Rieradevall, M., Reich, P., and Lake, P.S., 2013b. Effects of bushfire on macroinvertebrate communities in south-east Australian streams affected by a megadrought. Marine and Freshwater Research 65: 359-369.

Verkaik, I., Vila-Escale, M., Rieradevall, M., Baxter, C.V., Lake, P.S., Minshall, G.W., Reich, P. and Prat, N., 2015. Stream macroinvertebrate community responses to fire: are they the same in different fire-prone biogeographic regions? Freshwater Science, 34(4): 1527-1541.

Wells, W.W., 1987. The effects of fire on the generation of debris flows in southern California. In Costa, J.E., and Wieczorek, G.F., eds., Debris flows/avalanches: Processes, recognition, and mitigation: Reviews in Engineering Geology 7: I05-114.

Wells, W.W., Wohlgemuth, P. M., Campbell, A.G., 1987. Post-fire sediment movement by debris flows in the Santa Ynez Mountains, California. In Erosion and Sedimentation in the Pacific Rim: International Association of Hydrological Sciences Publication 165, p. 275-276.

Welsh, H.H., Ollivier, L.M., 1998. Stream amphibians as indicators of ecosystem stress: a case study from California's redwoods. Ecological Applications 8(4): 1118-1132.

Wester, T., Wasklewicz, T., Staley, D., 2014. Functional and structural connectivity within a recently burned drainage basin. Geomorphology 206: 362-373.

Westerling, A.L., Gershunov, A., Brown, T.J., Cayan, D.R. Dettinger, M.D., 2003. Climate and wildfire in the western United States. Bulletin of the American Meteorological Society 84(5): 595-604.

Westerling, A.L., Hidalgo, H.G., Cayan, D. R., Swetnam, T.W., 2006. Warming and earlier spring increase western U.S. forest wildfire activity. Science 313: 940-943.

Wheaton, J.M., Brasington, J., Darby, S.E. and Sear, D.A., 2010. Accounting for uncertainty in DEMs from repeat topographic surveys: improved sediment budgets. Earth Surface Processes and Landforms 35(2): 136-156.

Williams, K.E., Olsen, M.J., Chin, A., 2012. Accuracy Assessment of Geo-Referencing Methodologies for Terrestrial Lidar Laser Scan Site Surveys. American Society for Photogrammetry & Remote Sensing (ASPRS) Annual Conference, Sacramento, California, March 19-23. 2012, 10p.

Wohlgemuth, P.M. 2015. Hillslope erosion and small watershed sediment yield before and after fire in southern California. pp. 977-986. In Proceedings of the 3rd Joint Federal Interagency Conference (10th Federal Interagency Sedimentation Conference and 5th Federal Interagency Hydrologic Modeling Conference), Washington, D.C., USA.

Wolman, M.G., 1954. A method of sampling coarse river-bed material. EOS, Transactions American Geophysical Union 35(6): 951-956.

Yerkes, R. F., Campbell, R. H., 1980. Geological map of east-central Santa Monica Mountains, Los Angeles County, California. U.S. Geological Survey Miscellaneous Investigations Series, Map I-1146, scale 1:24 000.

TABLE 1. Absolute Differences between 2013 and 2014 TLS Scans: Average ∆x, ∆y, and ∆z Measured in 10 Boulder Sample Areas

Sample id	2013 #points	2014 #points	Absolute Differences ∆x	∆y	∆z
1	14368	65268	0.000	0.004	0.016
2	21777	77908	0.009	0.016	0.014
3	22440	63353	0.010	0.009	0.001
4	4014	6732	0.002	0.003	0.003
5	11459	6680	0.001	0.015	0.017
6	2216	3267	0.016	0.017	0.014
7	1068	2317	0.013	0.007	0.005
8	3088	19957	0.005	0.001	0.005
9	2427	1026	0.001	0.002	0.001
10	1145	602	0.006	0.001	0.002

TABLE 2. Uncertainty Analysis: Average and Maximum RMSE and Average Bias in Comparison of Triangulated Surface to Point Cloud Data along Cross Sections (see Figure 3B).

2013			**2014**		
Average RMSE (m)	Maximum RMSE (m)	Average Bias (m)	Average RMSE (m)	Maximum RMSE (m)	Average Bias (m)
0.0056	.0090	0.0005	0.0054	.0010	-0.0003

*Positive values represent overestimations and negative values represent underestimations

TABLE 3. Average Pre- and Post-storm Channel Characteristics

	Pool depth (m)	Step height (m)	Step spacing (m)	Step D_{max} (mm)	D_{50} (mm)	D_{84} (mm)	Sorting σ (D_s) (mm)	τ_o / τ_c
Before 2014 storm	0.2	0.3	14.4	401	88	250	143	0.4
After 2014 storm	0	0	na	na	5.8	20.3	101	4.7
After 2015 storm	0	0	na	na	2.6	8.0	3.5	13.7

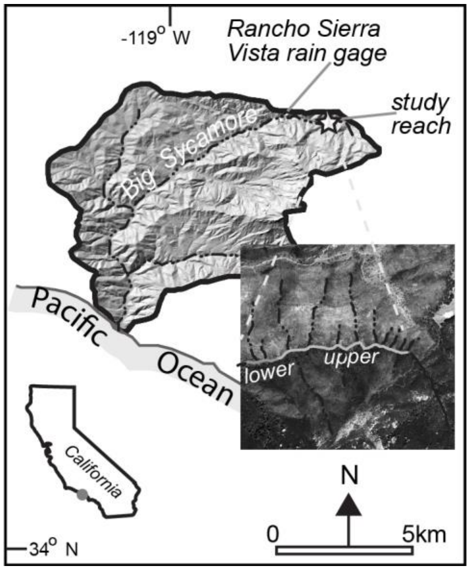

Figure 1. Location of Big Sycamore Creek in Southern California showing study reach and rain gage. Inset shows photograph of upper and lower portions of the study reach and tributaries comprising the channel network.

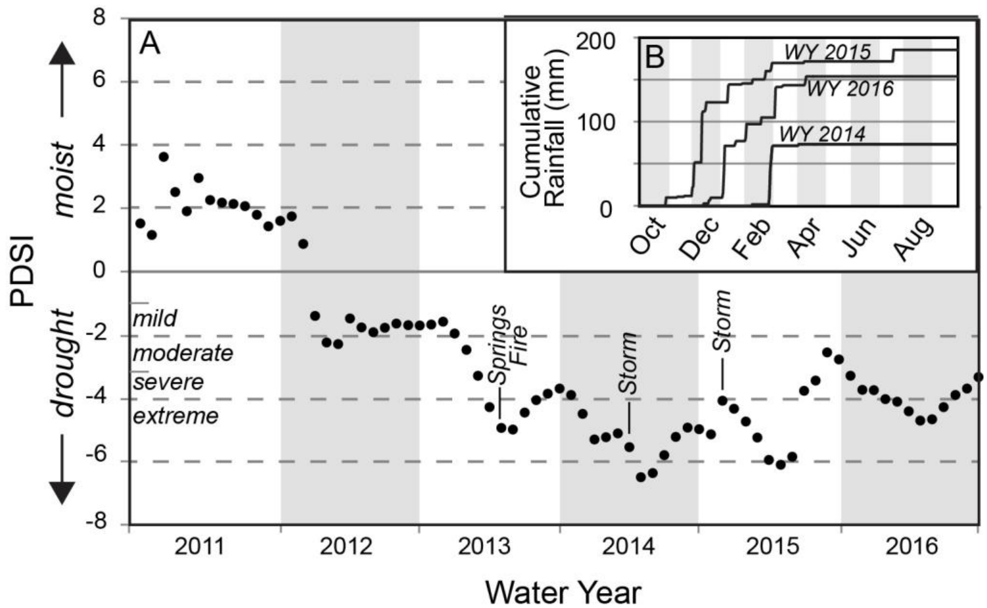

Figure 2A and 2B. (A) Palmer Drought Severity Index (PDSI) displays annual variability and temporal relation of the 2013 Springs Fire, WY 2014 and WY 2015 storms, and moisture conditions (data source: Desert Research Institute: www.wrcc.dri.edu). (B) Cumulative rainfall curve illustrates increases during all storms measured at Rancho Sierra Vista rain gage (see Figure 1; data source Ventura County Watershed Protection District (VCWPD) Hydrologic Data Server: www.vcwatershed.net/hydrodata/).

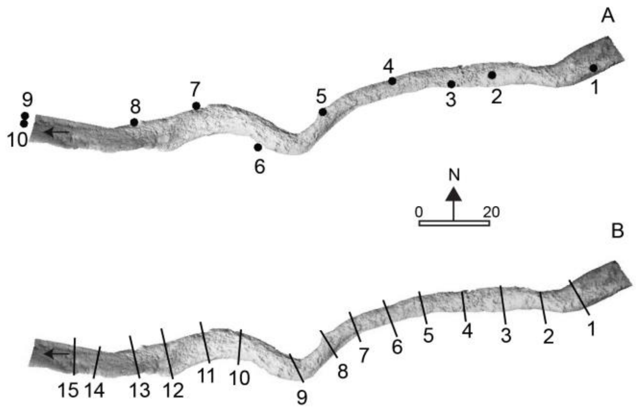

Figure 3A and 3B. Smoothed DEM derived from the 2014 TLS data**.** (A) Locations of large stationary rocks used for sampling elevation differences throughout the reach (upper image). (B) Location of cross sections used in uncertainty analysis to compare elevations of filtered point cloud data relative to triangulated surfaces in the TLS error analysis.

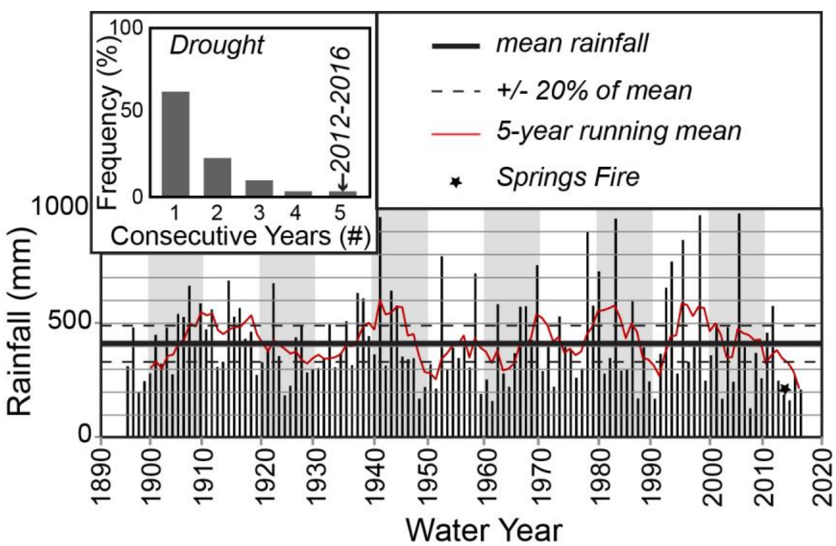

Figure 4. PRISM rainfall data for the period 1896 to 2016 illustrates annual variability. The five-year running mean corresponds to the temporal variability of ENSO in southern California. Inset shows frequency of droughts with one to five year durations—drought lasting one year is the most frequent; whereas, droughts with duration similar to the 2011-2016 drought have occurred only one other time over the period of record.

Figure 5. Photographs of the study reach before and after the 2014 storm, and after the 2015 storms.

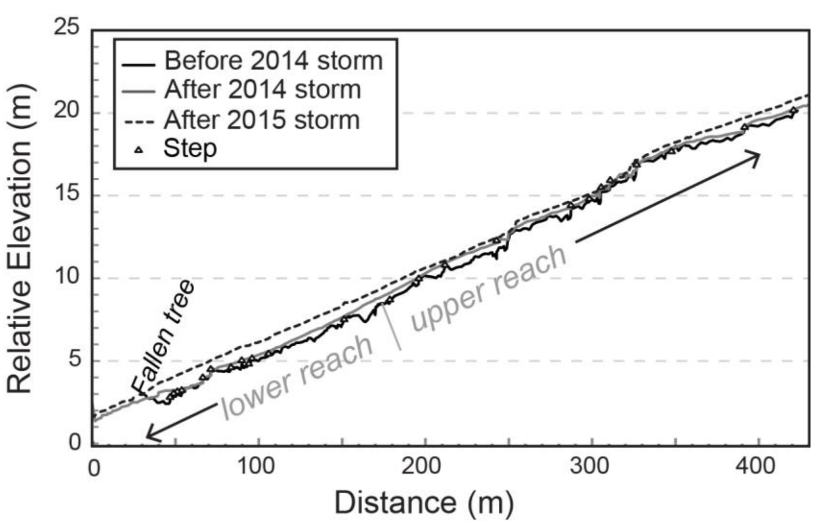

Figure 6. Longitudinal profiles before and after the 2014 storm and after the 2015 storms.

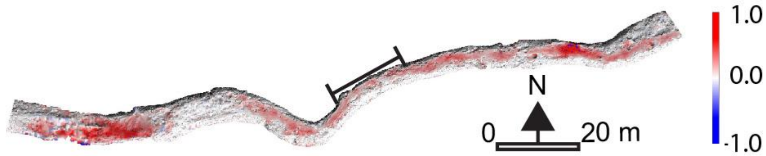

F**igure 7.** Volumetric change between 2013 and 2014 triangulated surfaces in the lower study reach. Bar indicates channel segment illustrated in Figure 8B.

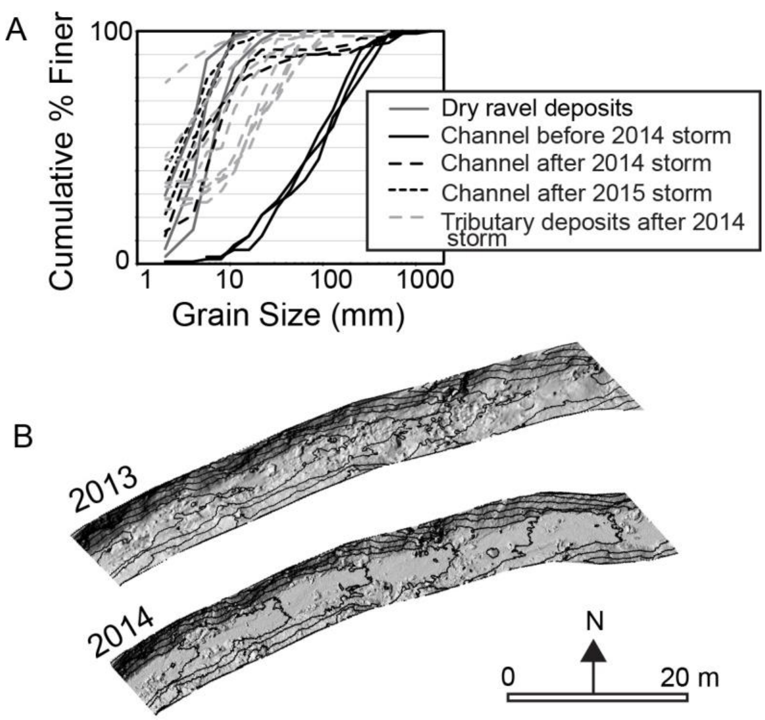

Figure 8A and 8B. Grain size distributions of material present on channel bed before and after storms, and dry ravel and tributary sediment contributions. (B) Sub-section of active channel DEM (see location on Figure 7) illustrates a relatively rough bed before the 2014 storm and smoother bed after sediment deposition during the storm. Contour Interval = 0.1m.